

# Robustness in sparse artificial neural networks trained with adaptive topology

Bendegúz Sulyok<sup>1</sup>, Gergely Palla<sup>1,2</sup>, Filippo Radicchi<sup>3</sup>, and Santo Fortunato<sup>3</sup>

<sup>1</sup>Dept. of Biological Physics, Eötvös Loránd University, Budapest, Hungary

<sup>2</sup>Semmelweis University, Faculty of Health and Public Administration, Health Services Management Training Centre, Budapest, Hungary

<sup>3</sup>Center for Complex Networks and Systems Research Luddy School of Informatics, Computing, and Engineering Indiana University Bloomington, USA

February 26, 2026

## Abstract

We investigate the robustness of sparse artificial neural networks trained with adaptive topology. We focus on a simple yet effective architecture consisting of three sparse layers with 99% sparsity followed by a dense layer, applied to image classification tasks such as MNIST and Fashion MNIST. By updating the topology of the sparse layers between each epoch, we achieve competitive accuracy despite the significantly reduced number of weights. Our primary contribution is a detailed analysis of the robustness of these networks, exploring their performance under various perturbations including random link removal, adversarial attack, and link weight shuffling. Through extensive experiments, we demonstrate that adaptive topology not only enhances efficiency but also maintains robustness. This work highlights the potential of adaptive sparse networks as a promising direction for developing efficient and reliable deep learning models.

## 1 Introduction

Deep Neural Networks (DNNs) have become the cornerstone of modern artificial intelligence, achieving state-of-the-art performance in diverse domains such as computer vision, natural language processing, and scientific computing [1, 2]. This success has been fueled by a trend of ever-increasing model size and complexity. Modern models often contain billions of parameters, leading to substantial computational and memory burden as well as significant energy cost for both training and inference [3]. This overparameterization not only poses significant challenges for deployment on resource-constrained devices like mobile phones and IoT sensors, but also raises environmental concerns regarding the carbon footprint of AI.

In parallel, the human brain provides an exceptionally efficient and powerful computational system for which neurological studies have long established that its connectivity is remarkably sparse [4, 5]. A typical neuron connects to only a vanishing fraction of other neurons, forming a complex yet highly efficient network structure. This biological sparsity is believed to be a key principle enabling the brain to learn and perform complex tasks with unparalleled energy efficiency [5, 6, 7]. This contrast between dense, computationally heavy artificial networks and the sparse, efficient biological brain drew considerable scientific interest towards sparsity in deep learning [8, 9, 10, 11, 12, 13, 14, 15].

However, it is worth noting that while artificial Sparse Neural Networks (SNNs) are significantly less connected than traditional dense models, they still retain a finite fraction of all the possible edges, meaning that they are not “sparse” in the jargon of network science [16]. On the other hand, real neural networks are sparse, as they display only a vanishing fraction of all possible connections. Despite this distinction, SNNs have emerged as a promising solution to mitigate the burdens of overparameterisation and are attractive for deployment on resource-constrained devices. By ensuring that a significant portion of the network’s weights are zero, SNNs can theoretically achieve dramatic reductions in storage requirements and computational complexity.

Seminal work in this area demonstrated that the sparsification of pre-trained dense models via network pruning can be achieved without a significant loss in the accuracy [8, 9]. More recent discoveries, such as the Lottery Ticket Hypothesis, suggest that sparse sub-networks with exceptional potential performance exist within dense models from the very beginning of the training [10]. Accordingly, in the pruning approach to SNN one starts from a fully connected neural network and gradually removes links while aiming to achieve an optimal balance between final performance and post-training inference speed [11, 12, 13, 14].

An equally important alternative to network pruning is the idea of sparse training, where a sparsely connected network is initiated, ensuring an inherent sparsity throughout the training [17, 18, 19, 20, 21, 22, 23]. A prominent approach in this direction is dynamic sparse training [17, 19, 20], which provides an efficient framework, where the network structure is also dynamically evolving during training. Epitopological learning is a variation of dynamic sparse training that is inspired by the plasticity of the brain and the way organic neural networks change their connectivity during learning, forming epitopological engrams (memory traces) [24, 25, 26, 27]. A relatively simple implementation of epitopological learning consists in applying link prediction during training, where one evaluates the likelihood of the existence of missing links based on the current network structure and takes this likelihood into account before the next modification to the network topology. In a slightly more general framework, epitopological learning can be implemented with the help of network automatons that provide connectivity predictions based on the input knowledge and the topological network organization.

Recently, a sparse network trained in the framework of Epitopological Sparse Meta-deep Learning (ESML) was shown to outperform fully connected networks across multiple architectures and datasets while retaining only 1% of the connections [28]. The basis of the framework was provided by the Cannistraci-Hebb (CH) automata learning theory, and the training procedure relied heavily on the CH3-CL network automata rules [29], offering an effective solution for general-purposed link prediction in bipartite networks.

In the present work, we examine this highly effective sparse neural network from the perspective of robustness. In the light of practical applications, robustness in neural networks is a critical concern, as models must perform reliably under various real-world conditions, including the presence of noise, adversarial perturbations, and shifts in data distribution. While sparsity can reduce overfitting and improve generalization, its impact on robustness is less understood, especially in the context of adaptive topologies. Here, we study the resilience of sparse neural networks trained in the ESML approach against various link removal procedures.

## 2 Results

### 2.1 Sparse architecture and training

The structure of the network architecture we used followed the setup proposed in Ref. [28], as illustrated in Fig. 1, showing the final stage of the training in one of our experiments with the MNIST dataset. The input layer consists of 784 pixels, which is followed by 3 sparsely connected neuron layers with 1000 neurons each. The network also contains an additional layer for readout, containing 10 neurons that are densely connected to the third layer.

The training of the network starts already with a sparse configuration, where only 1% of the possible connections are present between the input and the first 3 neuron layers, placed uniformly at random with a weight drawn from a normal distribution having a mean  $\mu = 0.0$  and a standard deviation  $\sigma = \sqrt{\frac{2}{f_{in}}}$ , where  $f_{in}$  is the size of the previous neuron layer. During the training in each epoch, first the weights are adjusted based on backpropagation. This is followed by rewiring of the connections, where first a small fraction of the links are deleted, and then an equal amount of new links are introduced to keep the overall number of connections in the network constant.

For the link regrowth procedure we applied two distinct strategies: Random Link Regrowth (RLR) and the CH3L3 heuristic [29, 28]. The RLR method, as its name suggests, assigns the new links simply at random. In contrast, the CH3L3 method is based on link prediction, where the new links are placed according to the highest likelihoods for unobserved connections in the current network topology. The two possible link regrowth strategies were not “mixed,” i.e., for any given experiment, one of the two possibilities was used exclusively throughout the entire training. In Fig. 2, we show the duration of the topology update for the two different link regrowth strategies. As expected, due to its simplicity,

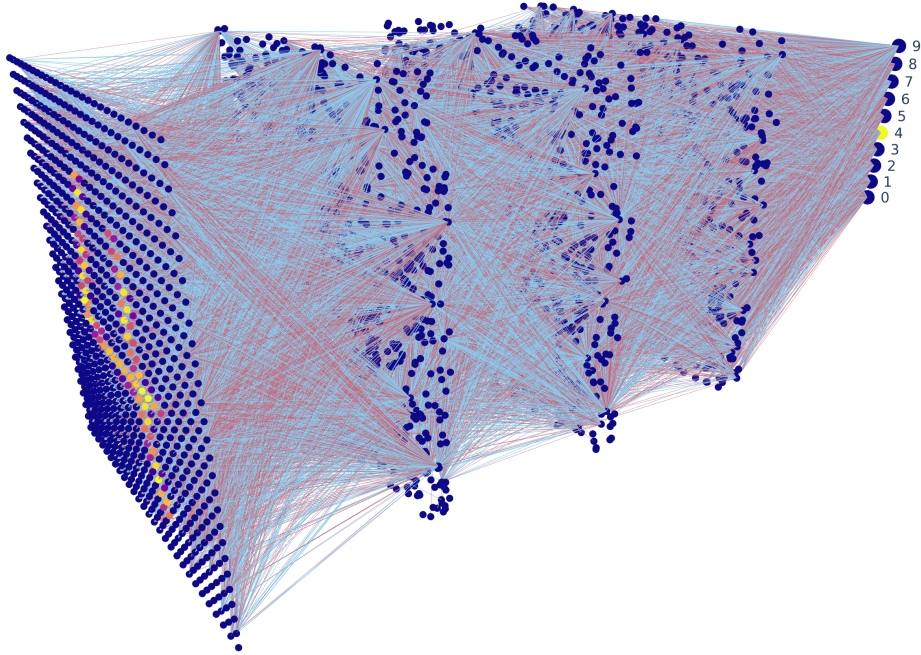


Figure 1: **Illustration of the network architecture.** The input layer (shown on the left) contains 28 x 28 pixels, followed by 3 sparsely connected neuron layers with 1000 neurons each. Blue coloured connections have a positive link weight, whereas red colour indicates a negative weight. The last layer, providing the readout is densely connected to the third sparse layer.

the RLR method roughly halves the average topology update time compared to the more complex CH3L3 method for all studied datasets. For a more detailed description of the training procedures, see Methods.

### 2.1.1 Accuracy

Figure 3 shows the evolution of test accuracy as a function of the training epochs for the MNIST (Fig.3a), Fashion MNIST (Fig.3b), KMNIST (Fig.3c), and EMNIST letters datasets (Fig.3d), where each curve represents the median over 10 independent training runs started from a different random seed. The shaded region around the curves falls between the 40<sup>th</sup> and 60<sup>th</sup> percentiles and indicates that a noticeable variability can be introduced by random initialization in the middle range of the training procedure for some systems.

For the studied datasets, the accuracy of the networks trained according to the CH3L3 method approaches its limiting value considerably faster compared to the accuracy of the networks trained with random link regrowth. However, the accuracy at the end of the training procedure is the same for both approaches within a short margin of uncertainty for all datasets except the KMNIST dataset (Fig.3c), where the maximal accuracy of the network trained with the CH3L3 method is slightly higher. Interestingly, in the case of the Fashion MNIST dataset (Fig.3b), after hitting a local maximum, the accuracy curve briefly decreases until reaching a local minimum, and then monotonically improves with each further training epoch for both training methods.

Put together, these results demonstrate that both training methods benefit from the alternating approach between weight update and link rewiring, and the applied sparse dynamic training framework is effective. In the meantime, the specific design of the update rule plays an important role in determining the speed of convergence.

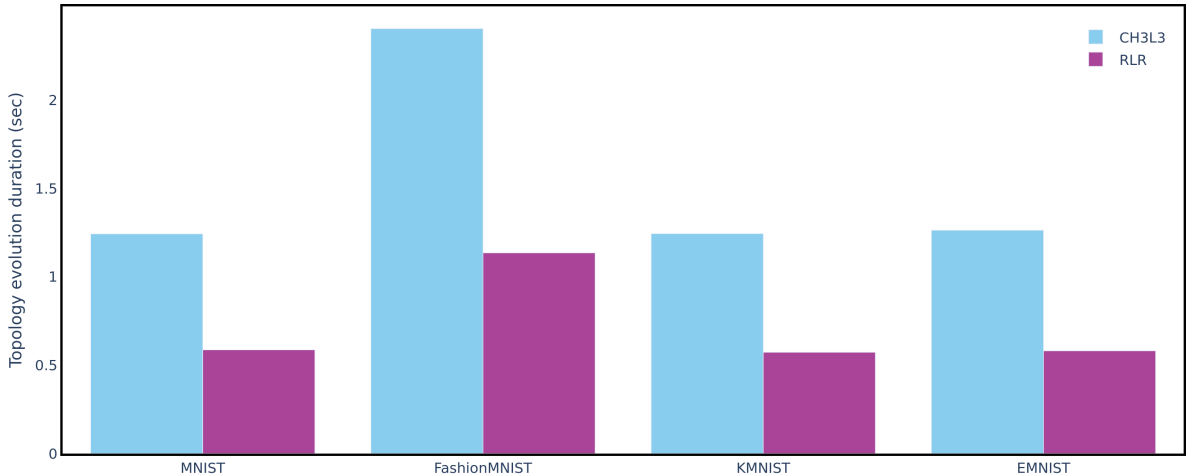


Figure 2: **Duration of the topology update.** We show the bar chart of the average duration in seconds for a single topology update over 4 training instances and 50 epochs. The results for the CH3L3 method are shown in light blue, whereas for the Random Link Regrowth method in purple, where the dataset is marked under the corresponding bars.

## 2.2 Robustness analysis

We assessed the robustness of the trained sparse networks through a systematic post-training perturbation analysis. After the completion of the training phase, we exposed the networks to two distinct types of disruption: iterative structural pruning (removing connections) and stochastic weight perturbation (randomly altering trained weights). The network performance was re-evaluated on the test set at each perturbation step, critically, without any subsequent fine-tuning or retraining.

The detailed list of the applied different types of perturbations is:

- *Random Pruning* - links are removed from the network layer-by-layer uniformly at random.
- *Weight Order Pruning* - links are removed by decreasing order of magnitude (i.e., highest-magnitude connections are removed first).
- *Reverse Weight Order Pruning* - links are removed in increasing order based on their weight magnitude.
- *Weight Shuffling* - weight values are shuffled within fixed-size bins applied layer-wise. The size of the perturbation is controlled by a value ranging from 0 to 1, which represents the ratio of the bin size by the total range of weight values within that layer. As this value increases, the bins become larger, allowing more disparate weight values to be shuffled together, thereby increasing the strength of the perturbation
- *Weight Modification* - random noise, sampled from a normal distribution centered on 0, is added to the weight values. The perturbation value  $m_p$  controls the standard deviation of the noise as  $\sigma_p = \bar{w} \cdot m_p$ , where  $\bar{w}$  is the average weight magnitude for the given layer.

In Fig.4 we show the accuracy as a function of the fraction of removed links for Random Pruning (green), Weight Order Pruning (gray) and Reverse Weight Order Pruning (red). As expected, for all tested datasets, the Weight Order Pruning decreases the performance of the networks in the most rapid fashion, with an almost vertical drop in the accuracy close to the origin, reaching the minimum value already at 1 to 5% of removed links. The studied sparse neural networks show more resilience against Random Pruning, where we can observe a gradual decrease in accuracy with roughly a constant (and finite) slope in the early stages of the link removal process, with steepness of the curves slightly reduced in the later stages, eventually decreasing to the minimum at around 80% removed links. Finally, the studied sparse dynamic neural networks show high resilience against Reverse Weight Order pruning, where accuracy may suffer only a minor decrease even at 80% of the links removed, which then is followed by a steep decline for larger fractions of removed links.

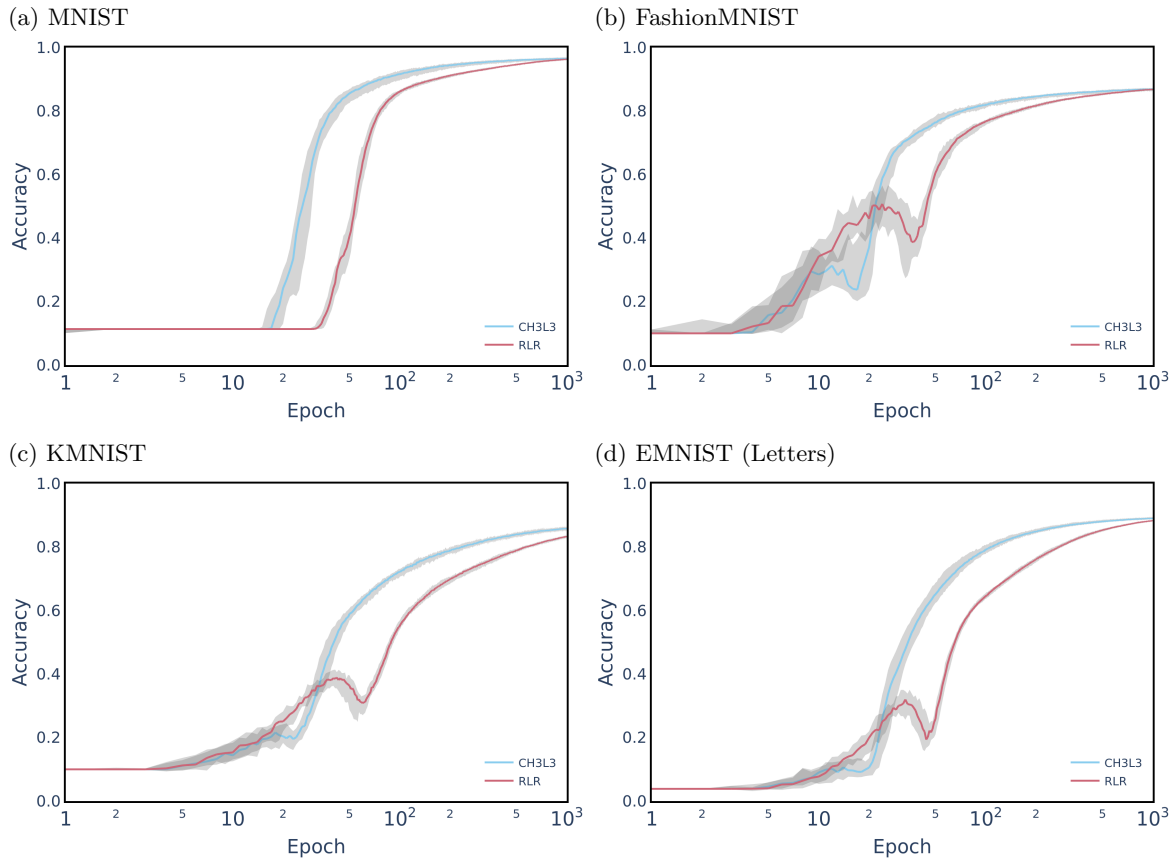


Figure 3: **Accuracy during training.** We show the accuracy (fraction of correctly classified inputs, where the shaded area indicates the standard deviation) as a function of the number of epochs (on logarithmic scale). The results for the *CH3L3* method are shown in blue, for the *Random Link Regrowth* method in red. Results are displayed for the following datasets: a) MNIST, b) FashionMNIST, c) KMNIST, and d) EMNIST Letters. Each setup was run 10 times with a different random seed and each training instance run for 1000 epochs with a topology update between consecutive epochs.

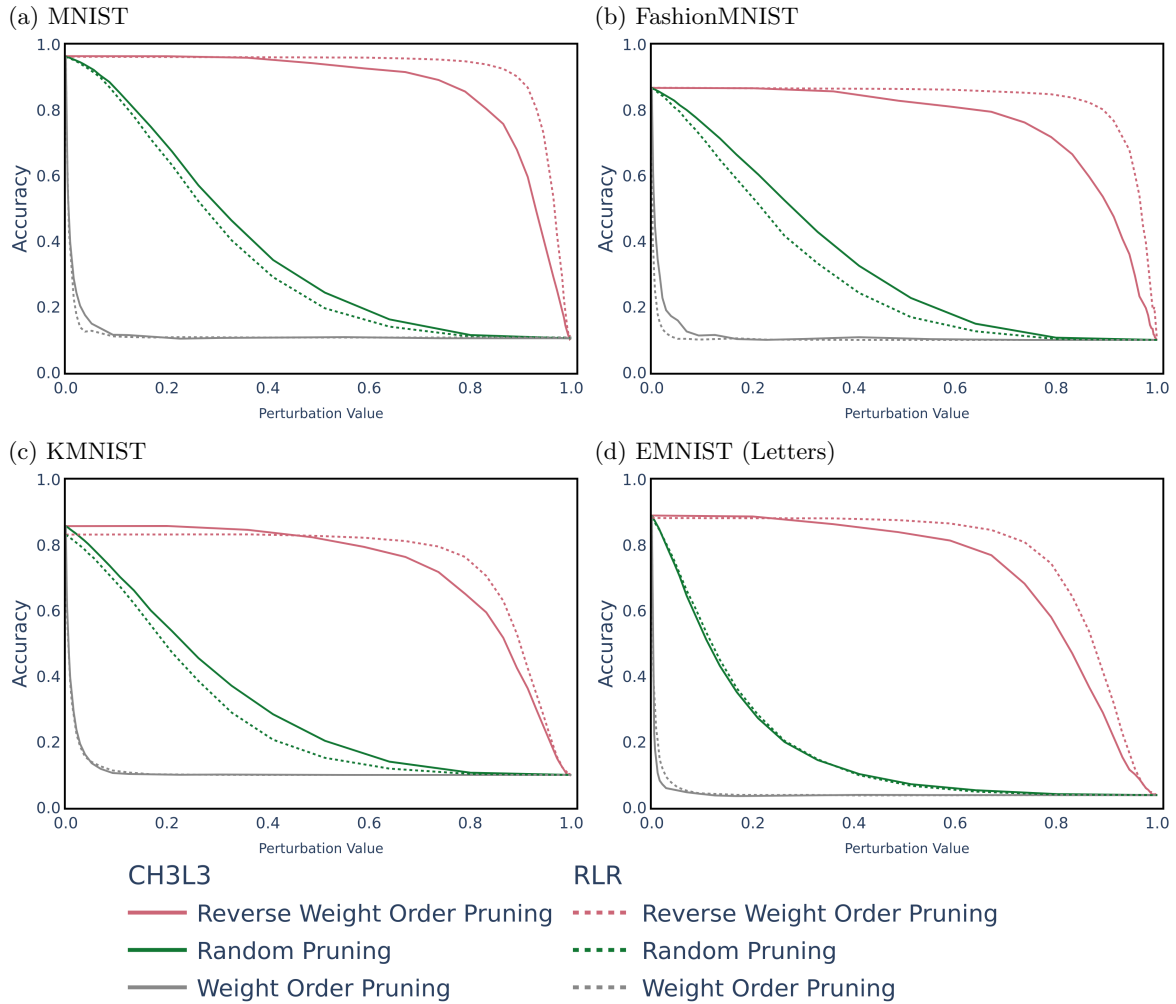


Figure 4: **Robustness of trained sparse networks against link removal.** Average accuracy over 32 networks as a function of the fraction of removed links (perturbation value) for systems trained according to the CH3L3 method (continuous lines) and the RLR method (dashed lines) for a) the MNIST dataset, b) the Fashion MNIST dataset, c) the KMNIST dataset, and d) the EMNIST letters dataset. Results for Reverse Weight Order Pruning are shown in red, for Random Pruning in green and for Weight Order Pruning in gray.

When comparing the robustness of the networks from the point of view of the two different training strategies, we can observe that networks trained with the RLR method (dashed lines) show higher resilience against Reverse Weight Order pruning for all datasets in Fig. 4. Resilience against Random Pruning yielded mixed results. Networks trained with the CH3L3 regrowth method showed slightly higher resilience across the MNIST, Fashion MNIST, and KMNIST datasets (Fig.4a-c). However, for the EMNIST letters dataset, the resilience curves for the two training strategies were nearly indistinguishable (Fig.4d). Finally, performance under Weight Order Pruning was dependent on the dataset. Networks trained using CH3L3 appeared slightly more resilient –though by a very small margin– for the MNIST and Fashion MNIST datasets (Fig.4a-b). Conversely, the RLR method resulted in slightly higher resilience for the KMNIST and EMNIST letters datasets (Fig.4c-d).

In Fig. 5 we show the decay of accuracy as a function of the perturbation value for Weight Shuffling (purple) and Weight Modification (light blue). Similarly to Fig. 4, curves plotted with continuous lines correspond to the results obtained for the networks trained with the CH3L3 link regrowth method, whereas results shown with dashed lines were obtained with the RLR method. For all tested datasets, the accuracy drops very fast for both types of perturbation, with the Weight Shuffling reducing the accuracy slightly even faster than the Weight Modification at the very start of the perturbation process. However, at some point the curves cross and in the later stages the accuracy for Weight Shuffling remains higher compared to that of Weight Modification. According to Fig.5, networks trained according to the CH3L3 method show slightly but noticeably stronger resilience against Weight Modification compared to networks trained with RLR in all tested datasets. In parallel, the comparison of the two training methods with respect to resilience against Weight Shuffling yields mixed results: Networks trained according to the CH3L3 method achieved higher robustness in the case of the MNIST and the FashionMNIST datasets (Fig.5a-b), whereas in the case of the KMNIST and the EMNIST Letters datasets it is the other way around (Fig.5c-d).

To investigate potential structural differences between networks trained using the CH3L3 algorithm and the RLR method, we measured the link weight distribution upon completion of the training processes, with Fig. 6 displaying the resulting density distributions of the weight magnitude across the various datasets. For all datasets and both training methods, we observe a narrow and pronounced local minimum in the density distribution near the origin. This is a consequence of the repeated link removal in each epoch, where a fixed fraction of the connections –specifically the weakest links– is consistently pruned. The steep decay immediately to the left of this minimum is primarily attributed to new links inserted in the final epoch, as these are initialized with weights drawn from a normal distribution centered at zero. Following this local minimum, a similarly narrow global maximum can be observed, and the density curves then proceed with a near-exponential decay towards larger weight values. When comparing the two training methods, the distributions show a consistent difference within the intermediate and moderately large weight range: specifically, in the range of approximately  $w = 0.2$  to  $w = 1$ , the density curves for networks trained with RLR (red lines) consistently exceed those for networks trained with the CH3L3 algorithm (light blue lines) across all datasets. However, the results for extremely large and rare weights ( $w > 1$ ) vary by dataset: the density for CH3L3 networks was higher than for RLR networks in the MNIST (Fig. 4a) and EMNIST datasets (Fig. 4d), was lower than for RLR networks in the Fashion MNIST dataset (Fig. 4b), and was roughly equal for the KMNIST dataset (Fig. 4c).

The measured properties of the weight magnitude densities, coupled with the assumption that connections with large weights contribute more significantly to network accuracy, offer a qualitative explanation for the observed robustness differences. Networks trained with RLR exhibit a higher density of medium-to-moderately-large weights compared to CH3L3 networks. Consequently, when both network types are subjected to Reverse Weight Order Pruning, the RLR networks retain larger weights among their remaining connections for any given fraction of links removed. This structural difference is expected to translate into superior performance and resilience for RLR-trained networks under RWO Pruning. Conversely, when links are removed randomly, the higher density of important, medium-to-moderately-large weights in RLR networks makes them more vulnerable to damage, resulting in a larger performance degradation compared to the CH3L3-trained networks at the same removal fraction.

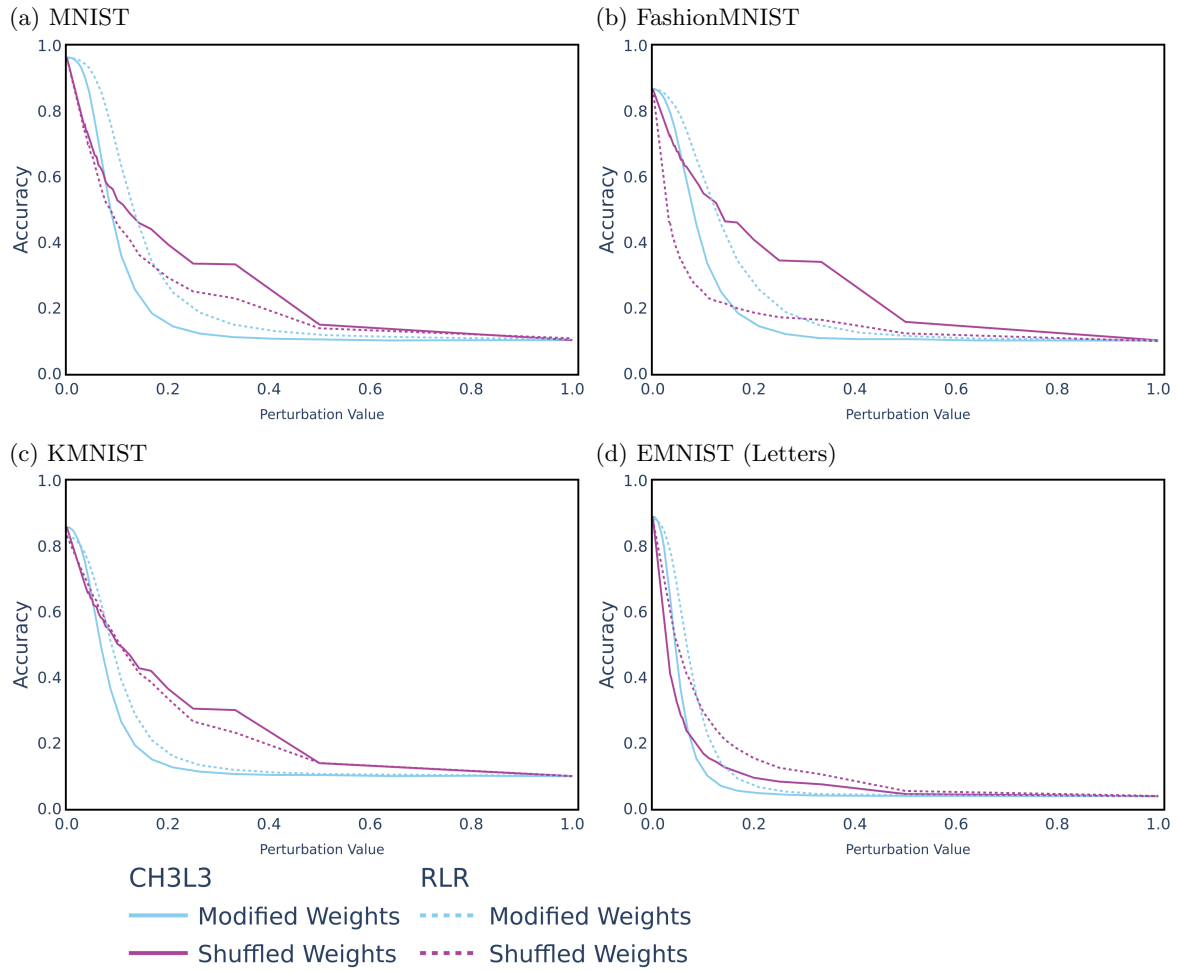


Figure 5: **Robustness of trained sparse networks against perturbing the weights by shuffling or adding noise.** Accuracy as a function of the perturbation value for networks trained with the CH3L3 Link Regrowth method (continuous lines) and with the RLR method (dashed lines) for a) the MNIST dataset, b) the Fashion MNIST dataset, c) the KMNIST dataset, and d) the EMNIST letters dataset. Results for Weight Shuffling are shown in purple, for Weight Modification in light blue.

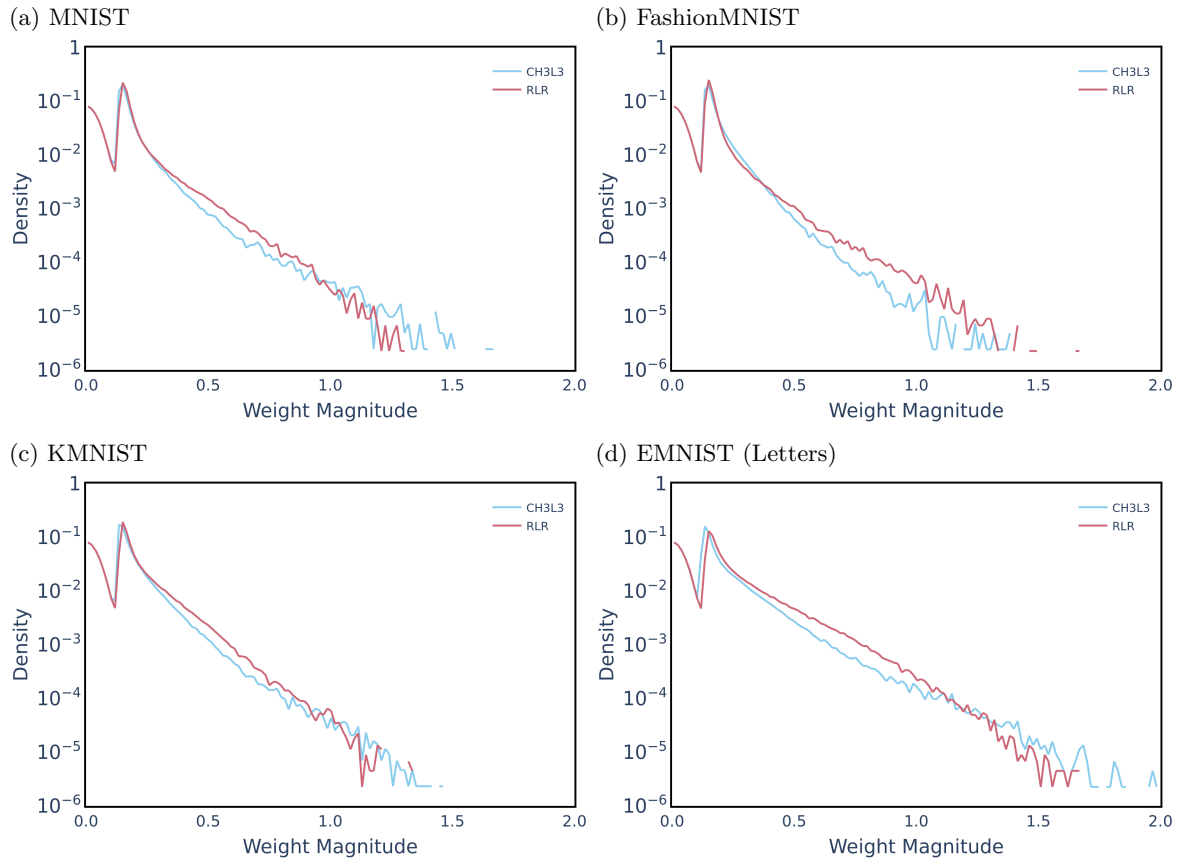


Figure 6: **Weight magnitude distribution in the trained networks.** We plot the distribution density for the absolute value of the connection weights at the end of the sparse training process, where results for networks trained according to the CH3L3 algorithm are shown in light blue and results for networks trained with RLR are shown in red. Panels depict the distributions observed for a) the MNIST dataset, b) the FashionMNIST dataset, c) the KMNIST dataset, and d) the EMNIST letters dataset.

### 3 Discussion

The study of network robustness, often framed as an inverse percolation process, where the network structure is incrementally deteriorated through subsequent link removal, has a long history in network science [30, 31]. Depending on the initial network structure and the specific perturbation applied, at a certain point the system may easily undergo a drastic change analogous to a phase transition in statistical physics. Such percolation transitions have been observed both in living neural networks, when chemically blocking neurotransmitter receptors [32], and in simulated neural networks, where resilience against various attacks strongly depended on the underlying architecture. The sequential pruning of connections is also a crucial method for compression in artificial neural networks, allowing an initially dense network to be converted into a sparse one while retaining near-original performance, despite the loss of the majority of its connections.

Relatedly, in the present paper we investigated the consequences of pruning and weight perturbations in neural networks that are already sparse from the outset. The networks studied were trained on four distinct datasets using two alternative dynamic training methods: the CH3L3 method (in which a fixed fraction of connections are removed and then reintroduced based on missing link prediction in each epoch) and the Random Link Regrowth (RLR) method (where the removed links are reintroduced at random).

Analysis of the training dynamics revealed that, across all datasets, CH3L3 networks reached maximum accuracy after fewer training epochs compared to RLR networks, though the final convergence accuracy for both methods was consistently the same within a negligible margin. Regarding resilience, CH3L3 networks proved to be more resilient against random link removal for three of the four datasets, with the fourth dataset showing nearly identical accuracy decay curves for both methods. In contrast, RLR networks showed higher resilience against Reverse Weight Order removal across all datasets. This latter result is particularly notable as it demonstrates the potential for significant further sparsification in RLR-trained networks, allowing up to approximately 80% of the connections to be removed without a critical loss in accuracy. However, both network types were highly susceptible to Weight Order removal, with accuracy often reducing to its minimum value after the removal of only 3% to 10% of the links. Beyond link removal, we analysed the effects of direct weight modification, finding that RLR-trained networks exhibited slightly greater resilience against random noise added to the weight values, whereas CH3L3 networks proved more resilient against random weight shuffling in three out of the four tested datasets.

A qualitative explanation for these differences stems from the resulting weight distributions. Our results show that in RLR-trained networks, a higher proportion of the distribution is concentrated in the medium-to-high weight range compared to CH3L3 networks. Based on this structural difference, RLR networks are expected to show higher resilience under Reverse Weight Order Pruning (which preferentially removes small weights), while CH3L3 networks are expected to be more resilient against Random Pruning (which is more likely to disrupt the concentrated, critical weights in the RLR distribution).

In summary, our study of the robustness of dynamically trained sparse neural networks against link pruning and weight modification shows that the specific dynamic training method employed has a notable effect on network resilience. Furthermore, results reveal that RLR-trained networks possess a structural quality that allows for extensive post-training compressibility without a significant loss in accuracy.

### 4 Methods

Our approach is based on training sparse neural networks while dynamically modifying their connectivity structure during training. The overall procedure consists of two main components: (i) weight learning and (ii) topology update. These are applied in an alternating fashion throughout training.

#### 4.1 Architecture

We employ multiple sparse layers followed by a single dense layer. The size of the input layer is fixed by the problem we are solving, for instance the popular MNIST dataset consists of input images of  $28 \times 28$  pixels, this corresponds to input size of 784 after flattening the image. This is followed by a

certain number of hidden neuron layers, for all experiments in this study we used three layers of 1000 neurons unless otherwise specified. These hidden neurons are sparsely connected to the neurons of the preceding layer. Finally, the last layer of hidden neurons is densely connected to the output layer whose size is again specified by the problem at hand. MNIST has 10 classes, therefore this last dense layer contains  $1000 \times 10$  links. Each neurons on the hidden layers represent an aggregation (weighted sum) of incoming links and a ReLU activation function [33].

## 4.2 Initialization

We begin by initializing a sparse neural network with a predefined sparsity level. The initial connectivity pattern is created at random following the Erdős-Rényi random graph model. Of course, any other method can be used here. The weight parameters of the network are then initialized. The Kaiming initialization [34] is a popular option when working with ReLU activation, as it preserves the variance of activations during the forward pass and variance of gradients during the backward pass. In practice this is achieved by sampling weight values from the normal distribution  $N(0, 2/n_{in})$ , where  $n_{in}$  is the number of neurons of the previous layer (i.e. total number of possible incoming links). We are using Kaiming initialization unless otherwise mentioned.

## 4.3 Training Procedure

Training takes place in discrete epochs. Each epoch is composed of the following steps:

1. **Weight learning.** Given the current sparse connectivity, standard gradient-based optimization is applied to update the active parameters. During this step the network adapts its weight values according to the task at hand, conditioned on the present topology.
2. **Topology update.** After each epoch, the connectivity of the network is modified according to a specified update rule. The stages of the topology update are shown in Fig. 7.

One always starts with pruning (removing) links that are deemed irrelevant. In the simplest case we remove a predefined fraction of all existing links based on the magnitude of their weight values. This is motivated by the fact that connections with vanishing weight values tend to not contribute meaningfully to the activation of the neuron they feed into.

During an optional second pruning stage, we remove all disconnected neurons and their associated links. A neuron is considered disconnected if it does not lie on any directed path originating from the input layer and ending on the output layer. A link that is not connected to the output simply occupies precious space in the sparse network that could be used to house a meaningful link. Similarly, a link not connected to the input will at best have contributed to the activation of the neuron by a constant offset and should therefore be merged with the appropriate bias neuron.

Then, new links are grown. One may opt to introduce new links randomly or according to some heuristic. We analyzed trained sparse networks with a random rule – this is the method used in [PAPER FOR S.E.T. METHOD] – CH3L3 link prediction [PAPER for CH3L3] as well as simpler link prediction method based on counting the number of paths connecting two neurons.

Finally, the new links are initialized by sampling from a distribution. Here, again, we use Kaiming initialization unless otherwise specified.

By alternating between weight learning and topology updates, the network explores different sparse configurations over the course of training, potentially improving its ability to discover efficient and expressive structures.

## References

- [1] Alex Krizhevsky, Ilya Sutskever, and Geoffrey E. Hinton. Imagenet classification with deep convolutional neural networks. In Peter L. Bartlett, Fernando C. N. Pereira, Christopher J. C. Burges, Léon Bottou, and Kilian Q. Weinberger, editors, *Advances in Neural Information Processing Systems 25: 26th Annual Conference on Neural Information Processing Systems 2012. Proceedings of a meeting held December 3-6, 2012, Lake Tahoe, Nevada, United States*, pages 1106–1114, 2012.

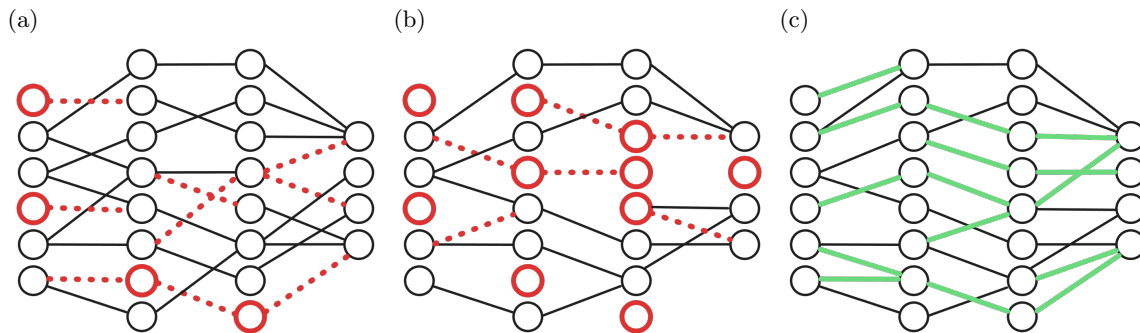


Figure 7: **The three stages of the topology update.** In the first stage (a) a fraction of links (dotted red lines) is removed in each sparse layer. In the second optional stage (b) all links that are no longer connected to the input and/or output layer (dotted red lines) are also removed. In the final stage (c) new links (green) are drawn and initialized such that the total number of links in each layer will be unchanged after the procedure.

- [2] Ashish Vaswani, Noam Shazeer, Niki Parmar, Jakob Uszkoreit, Llion Jones, Aidan N Gomez, Łukasz Kaiser, and Illia Polosukhin. Attention is all you need. In I. Guyon, U. Von Luxburg, S. Bengio, H. Wallach, R. Fergus, S. Vishwanathan, and R. Garnett, editors, *Advances in Neural Information Processing Systems*, volume 30. Curran Associates, Inc., 2017.
- [3] Emma Strubell, Ananya Ganesh, and Andrew McCallum. Energy and policy considerations for deep learning in NLP. In Anna Korhonen, David Traum, and Lluís Màrquez, editors, *Proceedings of the 57th Annual Meeting of the Association for Computational Linguistics*, pages 3645–3650, Florence, Italy, July 2019. Association for Computational Linguistics.
- [4] S. Ramón y Cajal. The croonian lecture.—la fine structure des centres nerveux. *Proceedings of the Royal Society of London*, 55:444–468, 1894.
- [5] V. Braitenberg and A. Schüz. *Cortex: Statistics and Geometry of Neuronal Connectivity*. Springer-Verlag, Berlin Heidelberg, 1998.
- [6] Babak Hassibi, David G. Stork, and Gregory J. Wolff. Optimal brain surgeon and general network pruning. *IEEE International Conference on Neural Networks*, pages 293–299 vol.1, 1993.
- [7] Bruno A. Olshausen and David J. Field. Sparse coding with an overcomplete basis set: A strategy employed by v1? *Vision Research*, 37(23):3311–3325, 1997.
- [8] Yann LeCun, John Denker, and Sara Solla. Optimal brain damage. In D. Touretzky, editor, *Advances in Neural Information Processing Systems*, volume 2. Morgan-Kaufmann, 1989.
- [9] Song Han, Jeff Pool, John Tran, and William Dally. Learning both weights and connections for efficient neural network. In C. Cortes, N. Lawrence, D. Lee, M. Sugiyama, and R. Garnett, editors, *Advances in Neural Information Processing Systems*, volume 28. Curran Associates, Inc., 2015.
- [10] Jonathan Frankle and Michael Carbin. The lottery ticket hypothesis: Finding sparse, trainable neural networks. In *7th International Conference on Learning Representations, ICLR 2019, New Orleans, LA, USA, May 6-9, 2019*. OpenReview.net, 2019.
- [11] Jiajun Li and Ahmed Louri. Adaprun: An accelerator-aware pruning technique for sustainable cnn accelerators. *IEEE Transactions on Sustainable Computing*, 7(1):47–60, 2022.
- [12] Mingjie Sun, Zhuang Liu, Anna Bair, and J. Zico Kolter. A simple and effective pruning approach for large language models, 2024.
- [13] Elias Frantar and Dan Alistarh. Sparsegpt: Massive language models can be accurately pruned in one-shot, 2023.

- [14] Yingtao Zhang, Haoli Bai, Haokun Lin, Jialin Zhao, Lu Hou, and Carlo Vittorio Cannistraci. Plug-and-play: An efficient post-training pruning method for large language models. In *The Twelfth International Conference on Learning Representations*, 2024.
- [15] Ziming Liu, Eric Gan, and Max Tegmark. Seeing is believing: Brain-inspired modular training for mechanistic interpretability. *Entropy*, 26(1), 2024.
- [16] Mark Newman. *Networks*. Oxford university press, 2018.
- [17] Decebal Constantin Mocanu, Elena Mocanu, Peter Stone, Phuong H. Nguyen, Madeleine Gibescu, and Antonio Liotta. Scalable training of artificial neural networks with adaptive sparse connectivity inspired by network science. *Nature Communications*, 9, 2017.
- [18] Namhoon Lee, Thalaiyasingam Ajanthan, and Philip Torr. SNIP: SINGLE-SHOT NETWORK PRUNING BASED ON CONNECTION SENSITIVITY. In *International Conference on Learning Representations*, 2019.
- [19] Utku Evci, Trevor Gale, Jacob Menick, Pablo Samuel Castro, and Erich Elsen. Rigging the lottery: Making all tickets winners. In *Proceedings of the 37th International Conference on Machine Learning, ICML 2020, 13-18 July 2020, Virtual Event*, volume 119 of *Proceedings of Machine Learning Research*, pages 2943–2952. PMLR, 2020.
- [20] Geng Yuan, Xiaolong Ma, Wei Niu, Zhengang Li, Zhenglun Kong, Ning Liu, Yifan Gong, Zheng Zhan, Chaoyang He, Qing Jin, Siyue Wang, Minghai Qin, Bin Ren, Yanzhi Wang, Sijia Liu, and Xue Lin. Mest: Accurate and fast memory-economic sparse training framework on the edge, 2021.
- [21] Geng Yuan, Yanyu Li, Sheng Li, Zhenglun Kong, Sergey Tulyakov, Xulong Tang, Yanzhi Wang, and Jian Ren. Layer freezing & data sieving: Missing pieces of a generic framework for sparse training, 2022.
- [22] Yuxin Zhang, Mingbao Lin, Mengzhao Chen, Fei Chao, and Rongrong Ji. Optg: Optimizing gradient-driven criteria in network sparsity, 2022.
- [23] Yuxin Zhang, Yiting Luo, Mingbao Lin, Yunshan Zhong, Jingjing Xie, Fei Chao, and Rongrong Ji. Bi-directional masks for efficient n:m sparse training, 2023.
- [24] Simone Daminelli, Josephine Maria Thomas, Claudio Durán, and Carlo Vittorio Cannistraci. Common neighbours and the local-community-paradigm for topological link prediction in bipartite networks. *New Journal of Physics*, 17(11):113037, nov 2015.
- [25] Claudio Duran, Simone Daminelli, Josephine M Thomas, V Joachim Haupt, Michael Schroeder, and Carlo Vittorio Cannistraci. Pioneering topological methods for network-based drug–target prediction by exploiting a brain-network self-organization theory. *Briefings in Bioinformatics*, 19(6):1183–1202, 2017.
- [26] Vaibhav Narula, Anders S Sørensen, Josephine M Thomas, Carlo Vittorio Cannistraci, Jay A Sankar, Christian A Jurgens, Anne E Raftery, and Anders Eklund. Can local-community-paradigm and epitopological learning enhance our understanding of how local brain connectivity is able to process, learn and memorize chronic pain? *Applied Network Science*, 2(1):48, 2017.
- [27] Carlo Vittorio Cannistraci. Modelling self-organization in complex networks via a brain-inspired network automata theory improves link reliability in protein interactomes. *Scientific Reports*, 8(1), oct 2018.
- [28] Yingtao Zhang, Jialin Zhao, Wenjing Wu, Alessandro Muscoloni, and Carlo Vittorio Cannistraci. Epitopological learning and cannistraci-hebb network shape intelligence brain-inspired theory for ultra-sparse advantage in deep learning. In *The Twelfth International Conference on Learning Representations*, 2024.
- [29] Alessandro Muscoloni, Umberto Michieli, and Carlo Vittorio Cannistraci. Adaptive network automata modelling of complex networks, December 2020.

- [30] R. Albert, H. Jeong, and AL. Barabási. Error and attack tolerance of complex networks. *Nature*, 406:378–382, 2002.
- [31] Oriol Artime, Marco Grassia, Manlio De Domenico, James P. Gleeson, Hernán A. Makse, Giuseppe Mangioni, Matjaž Perc, and Filippo Radicchi. Robustness and resilience of complex networks. *Nature Reviews Physics*, 6(2):114–131, February 2024.
- [32] Ilan Breskin, Jordi Soriano, Elisha Moses, and Tsvi Tlusty. Percolation in living neural networks. *Phys. Rev. Lett.*, 97:188102, Oct 2006.
- [33] Vinod Nair and Geoffrey E Hinton. Rectified linear units improve restricted boltzmann machines. In *Proceedings of the 27th international conference on machine learning (ICML-10)*, pages 807–814, 2010.
- [34] Kaiming He, Xiangyu Zhang, Shaoqing Ren, and Jian Sun. Delving deep into rectifiers: Surpassing human-level performance on imagenet classification. In *Proceedings of the IEEE international conference on computer vision*, pages 1026–1034, 2015.